



Research Article

Effect of calcination on the physical, chemical, morphological, and cementitious properties of red mud

Chava VENKATESH* , Cheretty SONALI SRI DURGA

Department of Civil Engineering, CVR College of Engineering, Vastunagar, Mangalpalli, Ibrahimpatnam-501510, Ranga Reddy, Telangana, India

ARTICLE INFO

Article history

Received: 16 October 2023

Revised: 16 November 2023

Accepted: 26 November 2023

Key words:

Compressive strength, particle analyzer, red mud, strength activity index, x-ray diffraction analysis

ABSTRACT

Red mud (RM), a by-product of aluminum production, poses environmental concerns with its disposal. This study explored calcining RM at 600 °C for 0–6 hours to utilize it as a cement substitute. Calcination up to 2 hours decreased particle size and increased surface area due to moisture loss, while further calcination reversed these effects. XRF analysis showed high Fe₂O₃, Al₂O₃, SiO₂ contents. XRD revealed goethite transformed to hematite and gibbsite to alumina. SEM images displayed a loose then denser structure over time. 10% calcined RM incorporated into cement showed 2-hour calcined RM exhibited optimal properties, including high strength (46.27 MPa) and strength activity index (117.24%). SEM confirmed improved C-S-H gel formation with 2-hour calcined RM. In summary, calcining RM optimally at 600 °C for 2 hours allows its effective use as a sustainable cementitious material, providing environmental and technical benefits of RM utilization in cement composites.

Cite this article as: Venkatesh, C., & Sonali Sri Durga, C. (2023). Effect of calcination on the physical, chemical, morphological, and cementitious properties of red mud. *J Sustain Const Mater Technol*, 8(4), 297–306.

1. INTRODUCTION

In recent years, there has been a growing emphasis on the development of novel technologies to transform waste into value-added products, particularly within industrial and mining sectors. This is due to the increased recognition that reducing waste is a significant environmental concern. By recycling these industrial products, it is possible to mitigate potential environmental and health-related complications, as well as enhance sustainability [1–3]. The present study is mainly focused on utilizing alumina industrial residue (i.e., red mud) as a cementing material. Red mud is a semi-solid residue produced during the extraction of alumina from bauxite, known as the Bayer process, in alumina production. Specifically, for every tonne of alumina extracted, 1.5 tonnes of red mud is generated as a residue [4, 5].

According to the Alam [6] & Mymrin [7], 4 billion tonnes of red mud is accumulated on open lands. Additionally, more than 140 million tonnes of red mud is added to this accumulation from throughout the world every year. Disposal of this large amount of red mud is very difficult due to its alkaline nature and is uneconomical as it requires much land [8]. Moreover, this disposal creates several environmental problems, such as air, water, and land pollution. Recycling of red mud is limited due to its fineness and high alkalinity, which may create an environmental imbalance [9, 10]. Besides, as a waste product, RM does not incur any additional production costs nor does it increase emissions; rather, it decreases emissions from cement production. Utilizing RM as a substitute for cement not only addresses storage concerns but also has the potential to enhance concrete properties, provided that it is used in appropriate quantities [11].

*Corresponding author.

*E-mail address: chvenky288@gmail.com



There are mixed opinions regarding the potential of red mud as a cementing material in cement/concrete composites, based on its strength and durability properties. Nikbin [12] reported that red mud has low cementing activity and shows a negative impact on compressive strength. Therefore, the usage of red mud is limited to the construction of non-structural elements. Su & Li [13] study revealed that incorporating 10% RM resulted in a minor reduction in the compressive strength of concrete, whereas incorporating more than 10% led to a significant decrease. A study by Yang [14] examined cement mortars that were based on red mud. The researchers replaced red mud in varying amounts, ranging from 0% to 9%. The results showed that the addition of red mud increased the mortar's density and improved its compressive strength. According to Ghaleh-novi [15], the use of red mud in self-compacting concrete (SCC) resulted in a decrease of 10% and 20% in compressive strength when the red mud content was 7.5% and 10%, respectively. Similarly, Venkatesh [16] reported a 19% decrease in the compressive strength of concrete with the addition of 15% red mud. However, another study found that as the amount of red mud used in concrete increased, the concrete's strength decreased [17]. The decrease in strength can be attributed to the fact that replacing cement with red mud, which has low reactivity, reduces the amount of hydration products per unit volume. Contrarily, W. C. Tang et al. [18] replaced fly ash with red mud in concrete. The study found that as the replacement percentage of red mud increased, the compressive strength improved. Specifically, when 50% of the fly ash was replaced with red mud, higher compressive strength was observed along with good improvement in Interfacial Transition Zone (ITZ). Furthermore, XRD analysis showed the presence of hatrurite and larnite. For instance, many investigations have started using red mud as a secondary or tertiary cementitious material in both normal and geopolymer concretes. In their studies, researchers have blended red mud with various cementing materials, including Slag [19], Metakaolin [20, 21], Fly ash [22], GGBFS [23], Phosphogypsum [24], Granite powder, and marble powder [25], and silica fume [26]. When red mud blend with other cementing materials has shown the considerable improvement in their strength and durability than its individual usage.

Although using red mud to prepare cement and concrete has promising application prospects, the presence of sodium in red mud can be detrimental to the strength and durability of cement and concrete. As a result, the amount of red mud utilized must be carefully controlled, or alternatively, the red mud must undergo a process of dealkalization, which ultimately restricts its application in cement and concrete production [27]. The conventional methods of dealkalization, such as acid neutralization, water leaching, and wet carbonation, are efficient. However, they also reduce the reactivity of red mud and have a negative impact on the performance of concrete. High-temperature treatment is an efficient method for enhancing the reactivity of red mud, as it can decompose some of its inert phases, such as cancrinite, gibbsite, and aragonite, into reactive ones that can easily

dissolve in the pore solution [28]. According to Luo [29], the ideal temperature for calcination to completely decompose cancrinite and birnessite in red mud is 1000 °C for one hour, while Danner [30] indicated that calcination at 800 °C for 15 minutes significantly enhanced the reactivity of red mud while decreasing the solubility of sodium. Manfroi [31] performed a calcium hydroxide consumption test and found that calcination at temperature of 600 °C for one hour was the optimal temperature for activating the pozzolanic reactivity of red mud. Liu et al. [32] stated that red mud demonstrated its highest pozzolanic activity when it was calcined for 3 hours at a temperature of 600 °C, which was attributed to the development of poorly-crystallized Ca_2SO_4 . Therefore, the general consensus is that calcination is a necessary precondition for red mud to exhibit reactivity. Without calcination, red mud would remain chemically unreactive in Portland cement blends, potentially resulting in weakened strength.

Research significance: Between 2010 and 2023, a total of 6,350 research articles were published on red mud as a cementing material, but less than 50 articles focused on the effect of calcination on red mud (The data was collected from Google Scholar using the following search limitations: a custom range in years from 2010 to 2023, article type set to research articles, and the keyword 'red mud as cementing material'.) There are varying opinions on the ideal calcination temperature for red mud, as its chemical composition differs from one location to another. The red mud produced by Indian aluminium industries, in particular, has limited usage in cement and concrete production due to a lack of literature on its cementing properties. Addressing this research gap, the present study conducted a comprehensive investigation into the physical and chemical properties of red mud, as well as its cementing activity when calcined at temperatures ranging from 600 °C for 1 hour to 6 hours.

2. MATERIALS AND METHODS

2.1. Materials

The present study obtained red mud from the NALCO in Orissa, India, which was in the semi-solid form with 30–40% moisture content during collection. It was dried in a laboratory (approximately 30 °C) for 3 days and then ground in ball mills. OPC-53 Grade cement was used for compressive strength and strength activity index tests, and all properties were within the limits of ASTM C150 [33]. Specifically, the specific surface area was 300 m²/kg, and the specific gravity was 3.12. Table 1 illustrates the Non-calcined red mud (NC-RM) and cement chemical compositions. The fine aggregates were used in accordance with IS: 383–2016 [34] and Table 2 shows its physical properties.

2.2. Calcination Process

In this study, a high-temperature muffle furnace was used for the calcination of red mud (RM), and a heating rate of 10 °C/min was maintained throughout the calcination process. The RM was calcined at a temperature of 600 °C for 1–6 hours and it is cooled at ambient air temperature for 5 hours in the laboratory after which it was ground in ball mills.

Table 1. Chemical composition (weight %)

	SiO ₂	Fe ₂ O ₃	Al ₂ O ₃	CaO	MgO	Na ₂ O	TiO ₂	K ₂ O	LOI
OPC	21.26	4.81	4.99	63.71	1.32	0.36	–	0.38	3.17
NC-RM	13.98	21.37	20.97	4.49	0.39	8.12	11.87	3.6	15.21

Table 2. Physical properties of aggregates

	Specific gravity	% of water absorption	Fineness modulus	Bulk density
Fine aggregates	2.69	1.10	2.56	1.46

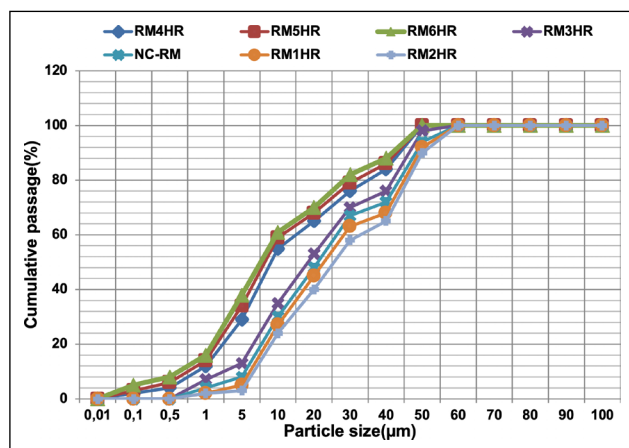


Figure 1. Particle size distribution of various calcined red muds.

2.3. Characterization Methods

In this study, the specific surface area of both calcined and non-calcined red mud samples was determined using the Micromeritics Gemini 237 and Gemini V instruments. Similarly, the particle size of the red mud samples was measured using the SZ-100Z nanoparticle analyzer from Horiba Ltd., Japan. The STA72000 thermal analyzer was used in this study to perform TG-DTA. Nitrogen (N₂) was used as a stripping gas, and all red mud samples were heated at a temperature range of 20 °C to 600 °C with a heating rate of 10 °C/min, as per Wu [35]. The Rigaku MiniFlex 600 with the following parameters was used to identify XRD patterns/phases: 40 kV voltage and 15 mA current, step scan of 0.0200°, scan range from 10° to 70° (2θ), a scan speed of 100.00 deg/min, and CuKα/1.541862 Å wavelength. VEGA 3 SBH, TESCAN Bmo. S.R.O., CZECH REPUBLIC, was used for identifying the surface morphology of calcined and non-calcined red mud samples. In the present study, the X'pert HighScore software tool has been used to analyze the XRD results, and it is supported by the new ICDD PDF-4+/Web licenses.

2.4. Mix Proportions

According to ASTM C109/C109M [36], the mix proportions of cement mortar samples are calculated, and the proportional ratios are as follows: 1:3:0.52 (i.e., binder: fine aggregates: water-to-cement ratio). In this study, 10% of various calcined red mud has been replaced with cement in all the mixes. A total of 48 mortar samples (with a size of 50 mm on each side of the cube) are prepared and cured for 7 and 28 days in portable water, following ASTM C31/C31M [37].

2.5. Strength Activity Index

The compressive strength and strength activity index (SAI) tests are evaluated on the red mud-induced cement mortar samples according to the ASTM C109/C109M [36] and ASTM C311/C311M [38] standards. Equation 1 is used to evaluate the strength activity index of red mud-induced cement mortar samples.

$$SAI(\%) = \frac{\text{Compressive strength of red mud induced cement mortar samples}}{\text{Compressive strength of normal cement mortar samples}} \times 100 \text{ Eq.1}$$

3. RESULTS AND DISCUSSION

3.1. Calcination Effect on Physical Properties of Red Mud

In this study, particle size analysis was conducted on the calcined red mud particles, as shown in Figure 1. The results show that all the red mud particles fall within the range of 1–50 µm, with an average particle size of 8 µm. The specific surface areas were measured using the BET apparatus and are illustrated in Table 2. Non-calcined red mud has a specific surface area of 1.86 m²/g, which increases to 2.2 m²/g after 2 hours of calcination. This increase is attributed to the loss of moisture in the particles and the destruction of alumina silicates present in the red mud particles, as mentioned by Liu [32]. They also state that specific surface area values decrease to 1.95 m²/g after 6 hours due to particle aggregation. According to Wu [35], the crystallinity of red mud particles increased with the enlargement of red mud particle size and the reduction in specific surface area resulting from calcination. Nath [39] have made similar conclusions, stating that particle size is enriched up to 200 °C of heating due to improved crystallinity. However, particle collision observed at a temperature of 500 °C leads to a reduction in particle size.

In this study, the specific gravity of red mud was measured according to IS 4031 Part-11 (1988) [40]. Table 3 illustrates the variations in the specific gravity of red mud when calcined at a temperature of 600 °C for 1 to 6 hours, and it is compared with non-calcined red mud. The specific gravity of red mud decreased by about 1.65% during 2 hours of calcination compared to non-calcined red mud, attributable to moisture loss in the particles. However, after 2 hours of calcination, the specific gravity values increased from 0.4% (at 3 hours) to 3.25% (at 6 hours). This effect can be attributed to agglomeration between the red

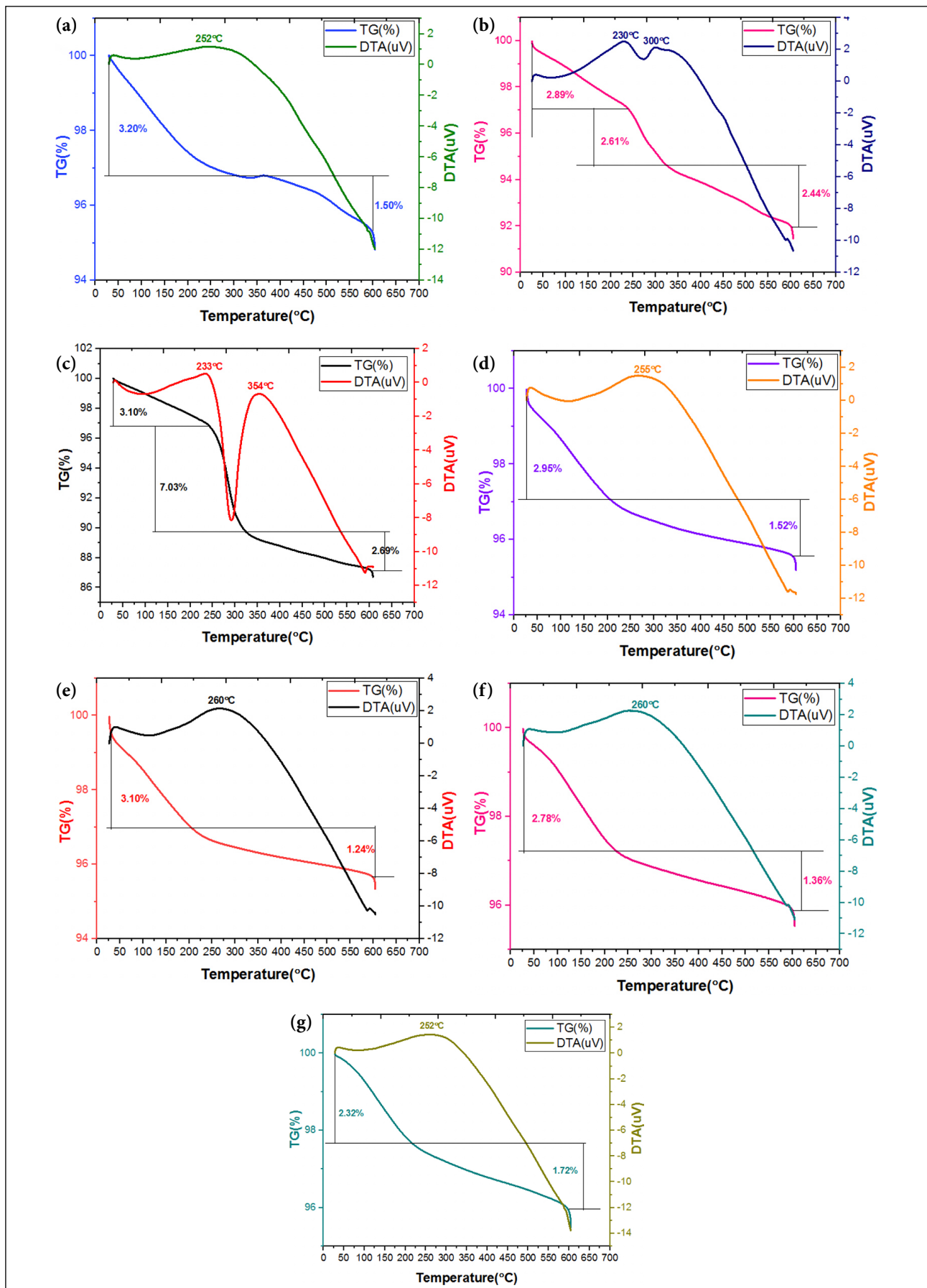


Figure 2. TG-DTA analysis of calcined red muds (a) NC-RM, (b) RM1HR, (c) RM2HR, (d) RM3HR, (e) RM4HR, (f) RM5HR and (g) RM6HR.

Table 3. Physical properties of red mud after calcination

	NC-RM	RM1HR	RM2HR	RM3HR	RM4HR	RM5HR	RM6HR
SSA (m ² /g)	1.86	1.95	2.2	2.16	2.1	2.05	1.95
Mass loss (%)	4.7	7.94	12.82	4.47	4.34	4.14	4.04
Specific gravity	2.46	2.44	2.42	2.47	2.5	2.51	2.54

Table 4. Chemical composition of calcined red mud (weight %)

Temp/time	CaO	Al ₂ O ₃	Fe ₂ O ₃	SiO ₂	Na ₂ O	K ₂ O	TiO ₂	MgO	LOI
NC-RM	4.49	20.97	21.37	13.98	8.12	3.6	11.87	0.39	15.21
RM1HR	7.53	26.15	22.54	17.6	5.44	3.03	7.92	0.84	8.95
RM2HR	10.84	22.62	21.79	21.92	3.87	1.89	5.5	0.65	10.92
RM3HR	9.66	24.63	22.47	19.82	5.03	2.48	6.72	0.92	8.27
RM4HR	8.44	21.08	24.01	19.46	5.81	2.19	7.01	1.26	10.74
RM5HR	8.54	22.54	24.06	18.47	8.24	2.27	7.19	0.41	8.28
RM6HR	12.3	20.2	21.46	16.89	10.35	2.22	8.17	0.33	8.08

mud particles Zhang [41] and Wang [42] reported that specific gravity values significantly varied when red mud was thermally activated.

In this study, thermogravimetry analysis was conducted on all calcined red mud particles to measure the mass loss, as shown in Table 3. Figure 2 depict the TG-DTA curves of all calcined red mud particles. The mass of the red mud particles varied with different calcination durations: 4.7% for non-calcined, 7.94% for 1 hour at 600 °C, 12.82% for 2 hours at 600 °C, 4.47% for 3 hours at 600 °C, 4.34% for 4 hours at 600 °C, 4.14% for 5 hours at 600 °C, and 4.04% for 6 hours at 600 °C. However, the reason for the mass loss observed up to 2 hours of calcination was attributed to dissipation of physical and chemically bound water.

Based on the obtained results, it was observed that all the physical properties, namely specific gravity, particle size, specific surface area, and mass loss, exhibited similar behavior. The calcination of red mud significantly influenced its physical properties. However, moisture loss was observed in the red mud for up to 2 hours of calcination. Subsequently, the physical properties were enhanced, which can be attributed to particle agglomeration.

3.2 Calcination Effect on Chemical Properties of Red Mud

Table 4 displays the chemical composition of red mud under different calcination durations at a temperature of 600 °C. Alumina, silica, and iron oxides were found to be the major components in all calcined red mud samples. Among them, the red mud subjected to a 2-hour calcination at 600 °C exhibited higher levels of silica and calcium oxide compared to the other calcined red mud samples. This increase in silica and calcium oxide content contributes to the enhanced cementitious activity of the red mud particles.

In this study, X-ray diffraction analysis was conducted to evaluate the phase transformations in red mud during calcination at a temperature of 600 °C for dif-

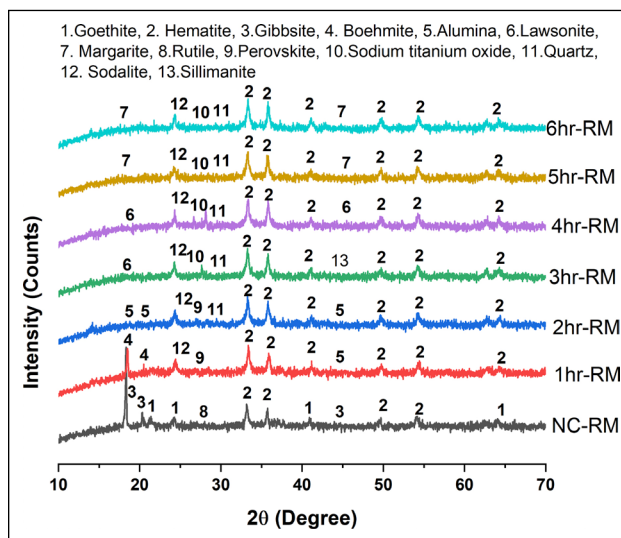


Figure 3. X-ray diffractogram of calcined red muds.

ferent durations (1 to 6 hours), as shown in Figure 3. The following mineralogical phases/compounds were identified: 1. Goethite (FeO(OH)), 2. Hematite (Fe₂O₃), 3. Gibbsite Al(OH)₃, 4. Boehmite (AlO(OH)), 5. Alumina-(Al₂O₃), 6. Lawsonite-(CaAl₂Si₂O₇(OH)₂(H₂O), 7. Margarite-(CaAl₂(Si₂Al₂O₁₀)(H₂O), 8. Rutile-(TiO₂), 9. Perovskite (CaTiO₃), 10. Sodium titanium oxide(Na₂TiO₃), 11. Quartz-(SiO₂), 12. Sodalite-(Na_{7.89}(AlSi₄)₆(NO₃)_{1.92}), 13. Sillimanite-(Al₂(SiO₄)O.

Gibbsite was observed at 2θ=14.47 with a d-spacing of 6.1215 in non-calcined red mud. However, after 1 hour of calcination at 600 °C, it transformed into boehmite due to moisture loss in the particles. Subsequently, boehmite further converted into alumina after 2 hours of calcination at 600 °C. Hematite showed no significant phase changes throughout all the calcined durations, with traced positions at 2θ=33.20, 35.68 and d-spacing of 2.6982, 2.5164. According to Nath [39], hematite remains stable up to 1200 °C.

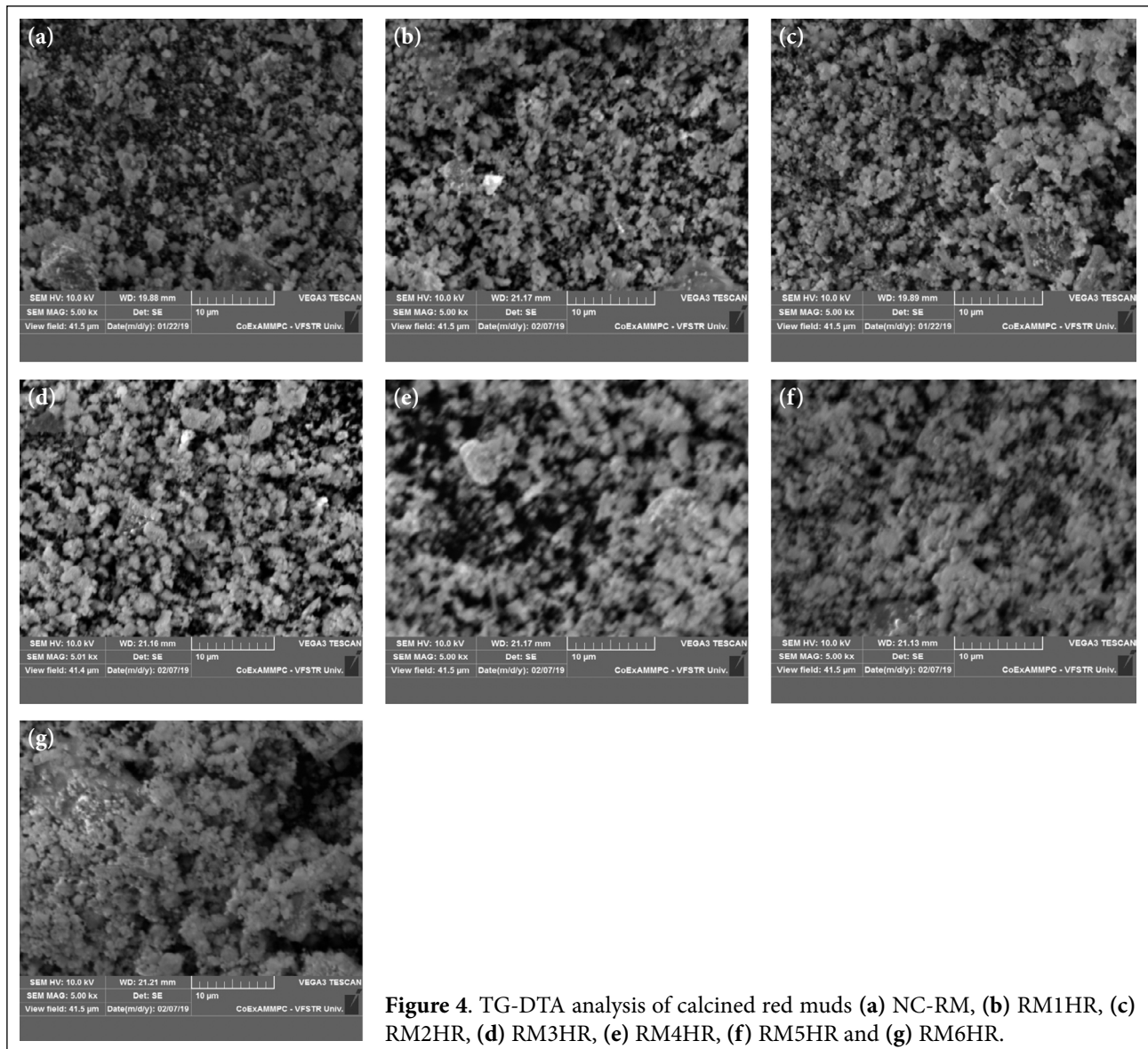


Figure 4. TG-DTA analysis of calcined red muds (a) NC-RM, (b) RM1HR, (c) RM2HR, (d) RM3HR, (e) RM4HR, (f) RM5HR and (g) RM6HR.

Table 5. Elemental composition of calcined red mud replaced mixes (weight %)

Mixes	28 days						Total
	O	Ca	Si	Al	Fe	Ca/Si	
NC-RM	56.51	22.69	16.91	3.19	0.7	1.34	100
RM1H	56.45	21.42	18.17	3.1	0.86	1.18	100
RM2H	58.71	18.2	19.19	3.09	0.81	0.95	100
RM3H	57.89	18.91	19.1	3.05	1.05	0.99	100
RM4H	61.01	21.05	15.25	2.24	0.45	1.38	100
RM5H	55.52	25.59	15	3.19	0.7	1.71	100
RM6H	55.52	24.42	16.1	3.1	0.86	1.52	100

Lawsonite transformed into sodalite, which explains the separation of calcium oxide during the calcination process. Rutile, initially present in the non-calcined red mud, changed to perovskite after 1 hour of calcination at 600 °C, and further calcination resulted in the complete transformation to sodium titanium oxide. S.N. Meher [43] also observed similar

phase transformations, from rutile to perovskite. This phase change suggests that the calcium oxide present in the red mud may react with titanium oxide and form perovskite (CaTiO_3).

Quartz was detected between 2 \square values of 25 to 30 in the 2-hour calcined red mud, and it continued to be present in further calcined red mud samples as well. The chemical

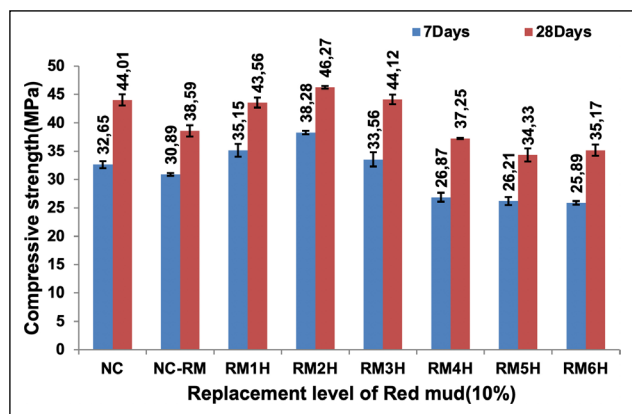


Figure 5. Compressive strength.

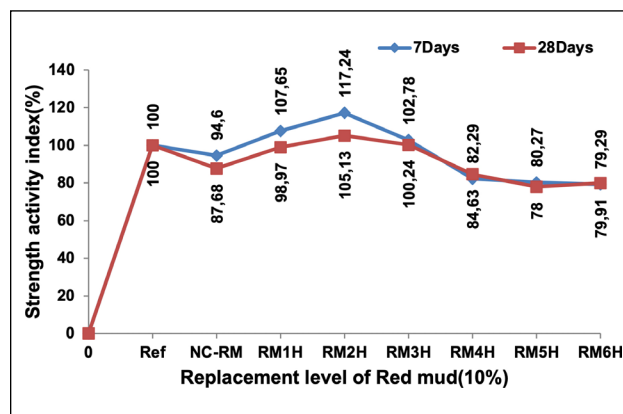


Figure 6. SAI Vs. Compressive strength.

composition results (mentioned in Table 3) also indicated the presence of stable or higher levels of silica (SiO₂) after 2 hours of calcination.

Scanning electron microscopy (SEM) analysis was conducted to examine the surface morphology of red mud particles during various calcination processes. Figure 4 illustrates the SEM images of different calcined red mud particles. Microscopic observations revealed that the red mud particles exhibit an irregular shape. However, up to 2 hours of heating at 600 °C, the red mud particles maintain a loose structure. In particular, Figure 4c shows a more poorly crystalline structure compared to others, which may indicate higher reactivity and better cementitious activity. A similar conclusion was made by Liu [32], stating that red mud forms a poorly crystalline structure when thermally activated, providing ideal cementitious activity. Subsequently, a dense structure is observed from 2 hours to 6 hours of heating at 600 °C as the particles undergo agglomeration, resulting in their combination with surrounding particles. Similar observations regarding the physical properties of red mud were made in this study.

3.4. Calcination Effect on Cementitious Properties of Red Mud

The present study conducted the strength activity index test according to ASTM C311/C311M [38] to investigate the cementitious properties of red mud particles. In this regard, the cement mortar mixes were prepared by replacing the 10% of cement by calcined red mud (Calcined at a temperature of 600 °C during 1 to 6 hours). The results showed that the cement mortar samples containing 600 °C@2hr (i.e., RM2HR) calcined red mud exhibited high strength, specifically 46.27 MPa, as shown in Figure 5. This effect can be attributed to the higher percentage of silica and the increased specific surface area of the red mud particles, which enhance the hydration process of the cementitious matrix.

Figure 6 illustrates the strength activity index percentages of calcined red mud induced cement mortar mixes; 107.65% for RM1HR, 117.24% for RM2HR, 102.78% for RM3HR, 82.29% for RM4HR, 80.27% for RM5HR, and 79.29% for RM6HR. According to the ASTM C311/C311M [38], Wang et al. [44] and [45, 46] If the strength activity index values exceed 75%, the material exhibits good cementi-

tious properties and is suitable for use as a cementitious material in concrete/mortar. Microstructure analysis revealed that red mud possesses significant cementitious properties as like cement. SEM images in Figure 7 indicate the formation of C-S-H (calcium silicate hydrate) and CH (calcium hydroxide). Notably, the cement mortar mixes with 2hr calcined red mud replacement exhibited better C-S-H gel formation than other mixes, as observed through the Ca/Si ratios in the elemental composition of red mud replaced mixes, as shown in Table 5. The RM2HR calcined red mud containing mortar mix has low Ca/Si of 0.95 this is the reason for achievement of high strength (i.e., 46.27 MPa) and strength activity index values (i.e., 117.24%). According to Rossignolo [47] and MSR Chand [48], the presence of C-S-H can be justified by the Ca/Si ratio of the EDXA (Energy-Dispersive X-ray Analysis) elemental weight percentages. A Ca/Si ratio ranging from 0.8 to 2.5 confirms the presence of C-S-H gel, while a lower Ca/Si ratio indicates a stronger or higher C-S-H gel formation Venkatesh [49].

4. CONCLUSIONS

In this study, red mud, a by-product of the Indian alumina industry (specifically NALCO), was calcined at a temperature of 600 °C for 1 to 6 hours to evaluate its potential usage as a cementing material in cement/concrete production. The following conclusions were drawn after comprehensive assessments of its physical, chemical, morphological, and cementing properties.

- Chemical evaluation studies have identified that red mud contains abundant amounts of silica, iron oxide, and alumina. In the case of calcined red mud at 600 °C for 2 hours (600 °C@2hr), it was found to contain 10.84% CaO, 21.92% SiO₂, and 22.62% alumina, making it more suitable as a cementing material.
- Based on the XRD analysis, hematite remained stable throughout the calcination process. However, gibbsite in non-calcined red mud transformed into boehmite at RM1HR, and further calcination at 600 °C for 2 hours resulted in its conversion into alumina.
- The RM2HR calcined red mud replacement mixes exhibited high compressive strength and strength activity index values, specifically 46.27 MPa and 117.24%. It

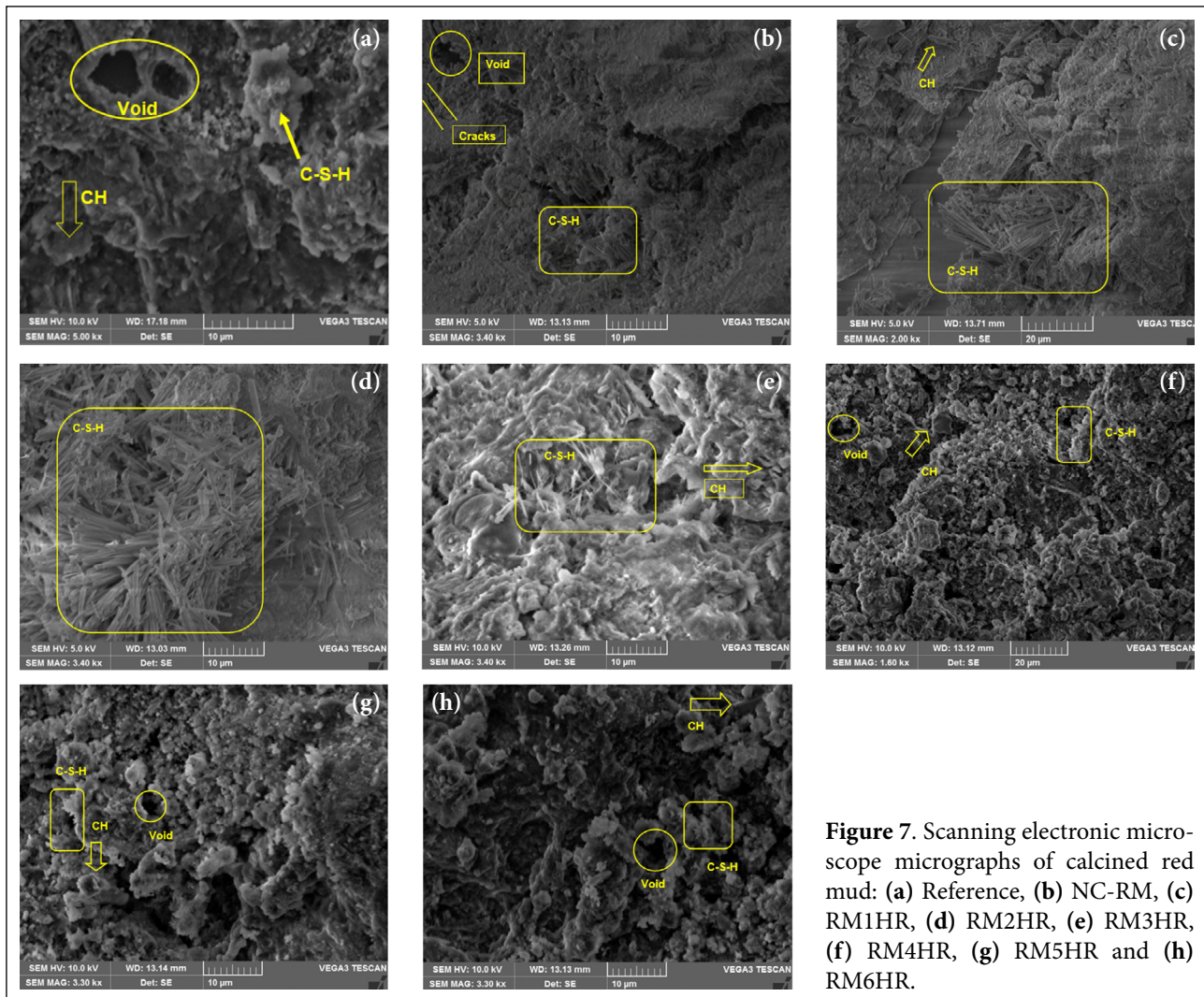


Figure 7. Scanning electronic microscope micrographs of calcined red mud: (a) Reference, (b) NC-RM, (c) RM1HR, (d) RM2HR, (e) RM3HR, (f) RM4HR, (g) RM5HR and (h) RM6HR.

was observed that this particular red mud contained a higher amount of silica (21.92%), a large specific surface area (2.2 m²/g), and a poorly crystalline structure. These factors played a positive role in the cementing activities.

- Finally, NALCO-produced red mud can be utilized as a cementing material in cement/concrete production after undergoing calcination at a temperature of 600 °C for 2 hours.

ETHICS

There are no ethical issues with the publication of this manuscript.

DATA AVAILABILITY STATEMENT

The authors confirm that the data that supports the findings of this study are available within the article. Raw data that support the finding of this study are available from the corresponding author, upon reasonable request.

CONFLICT OF INTEREST

The authors declare that they have no conflict of interest.

FINANCIAL DISCLOSURE

The authors declared that this study has received no financial support.

PEER-REVIEW

Externally peer-reviewed.

REFERENCES

- [1] Muraleedharan, M., & Nadir, Y. (2021). Factors affecting the mechanical properties and microstructure of geopolymers from red mud and granite waste powder: A review. *Ceram Int*, 47(10), 13257–13279. [CrossRef]
- [2] Çelikten, S., Atabey, İ. İ., & Bayer Öztürk, Z. (2022). Cleaner environment approach by the utilization of ceramic sanitaryware waste in Portland cement mortar at ambient and elevated temperatures. *Iranian J Sci Technol Trans Civ Eng*, 46(6), 4291–4301. [CrossRef]
- [3] Korkmaz, A. V., & Kayıran, H. F. (2022). Investigation of mechanical activation effect on high-volume natural pozzolanic cements. *Open Chem*, 20(1), 1029–1044. [CrossRef]
- [4] Gou, M., Hou, W., Zhou, L., Zhao, J., & Zhao, M. (2023). Preparation and properties of calcium aluminate cement with Bayer red mud. *Constr Build Mater*, 373, 130827. [CrossRef]

- [5] Venkatesh, C., Nerella, R., & Chand, M. S. R. (2020). Experimental investigation of strength, durability, and microstructure of red-mud concrete. *J Korean Ceram Soc*, 57(2), 167–174. [\[CrossRef\]](#)
- [6] Alam, S., Das, S. K., & Rao, B. H. (2019). Strength and durability characteristic of alkali-activated GGBS stabilized red mud as geo-material. *Constr Build Mater*, 211, 932–942. [\[CrossRef\]](#)
- [7] Mymrin, V., Alekseev, K., Fortini, O. M., Aibuldin-ov, Y. K., Pedroso, C. L., Nagalli, A., Winter, E. Jr., Catai, R. E. & Costa, E. B. C. (2017). Environmentally clean materials from hazardous red mud, ground-cooled ferrous slag, and lime production waste. *J Clean Prod*, 161, 376–381. [\[CrossRef\]](#)
- [8] Ortega, J. M., Cabeza, M., Tenza-Abril, A. J., Real-Herraiz, T., Climent, M. Á., & Sánchez, I. (2019). Effects of red mud addition in the microstructure, durability, and mechanical performance of cement mortars. *Appl Sci*, 9(5), 984. [\[CrossRef\]](#)
- [9] Liu, Z., & Li, H. (2015). Metallurgical process for valuable elements recovery from red mud - A review. *Hydrometallurgy*, 155, 29–43. [\[CrossRef\]](#)
- [10] Abdel-Raheem, M., Santana, L. G., Cordava, M. P., & Martínez, B. O. (2017). Uses of red mud as a construction material. In *AEI 2017* (pp. 388–399). [\[CrossRef\]](#)
- [11] Patangia, J., Saravanan, T. J., Kabeer, K. S. A., & Bisht, K. (2023). Study on the utilization of red mud (bauxite waste) as a supplementary cementitious material: Pathway to attaining sustainable development goals. *Constr Build Mater*, 375, 131005. [\[CrossRef\]](#)
- [12] Nikbin, I. M., Aliaghazadeh, M., Charkhtab, S. H., & Fathollahpour, A. (2018). Environmental impacts and mechanical properties of lightweight concrete containing bauxite residue (red mud). *J Clean Prod*, 172, 2683–2694. [\[CrossRef\]](#)
- [13] Su, Z., & Li, X. (2021). Study on preparation and interfacial transition zone microstructure of red mud-yellow phosphorus slag-cement concrete. *Mater*, 14(11), 2768. [\[CrossRef\]](#)
- [14] Yang, X., Zhao, J., Li, H., Zhao, P., & Chen, Q. (2017). Recycling red mud from the production of aluminium as a red cement-based mortar. *Waste Manag Res*, 35(5), 500–507. [\[CrossRef\]](#)
- [15] Ghalehnovi, M., Shamsabadi, E. A., Khodabakhshian, A., Sourmeh, F., & De Brito, J. (2019). Self-compacting architectural concrete production using red mud. *Constr Build Mater*, 226, 418–427. [\[CrossRef\]](#)
- [16] Venkatesh, C., Nerella, R., & Chand, M. S. R. (2020). Comparison of mechanical and durability properties of treated and untreated red mud concrete. *Mater Today: Proc*, 27, 284–287. [\[CrossRef\]](#)
- [17] Raja, R. R., Pillai, E. P., & Santhakumar, A. R. (2013). Effective utilization of red mud bauxite waste as a replacement of cement in concrete for environmental conservation. *Ecol Environ Conserv*, 19(1), 247–255.
- [18] Tang, W. C., Wang, Z., Liu, Y., & Cui, H. Z. (2018). Influence of red mud on fresh and hardened properties of self-compacting concrete. *Constr Build Mater*, 178, 288–300. [\[CrossRef\]](#)
- [19] Li, Z., Zhang, J., Li, S., Gao, Y., Liu, C., & Qi, Y. (2020). Effect of different gypsums on the workability and mechanical properties of red mud-slag based grouting materials. *J Clean Prod*, 245, 118759. [\[CrossRef\]](#)
- [20] Liu, J., Li, X., Lu, Y., & Bai, X. (2020). Effects of Na/Al ratio on mechanical properties and microstructure of red mud-coal metakaolin geopolymer. *Constr Build Mater*, 263, 120653. [\[CrossRef\]](#)
- [21] Raj, R. R., Pillai, E. P., & Santhakumar, A. R. (2012). Strength and corrosion properties of concrete incorporating metakaolin and red mud. *Eur J Sci Res*, 91(4), 569–579.
- [22] Qaidi, S. M., Tayeh, B. A., Ahmed, H. U., & Emad, W. (2022). A review of the sustainable utilization of red mud and fly ash for the production of geopolymer composites. *Constr Build Mater*, 350, 128892. [\[CrossRef\]](#)
- [23] Zhao, Y., Zhang, B., He, F., Meng, F., Yang, S., Wang, Q., & Zhu, W. (2023). Effects of dosage and type of GGBS on the mechanical properties of a hybrid red-mud geopolymer. *J Mater Civ Eng*, 35(4), 04023008. [\[CrossRef\]](#)
- [24] Huang, X., Li, J. S., Jiang, W., Chen, Z., Wan, Y., Xue, Q., Liu, L. & Poon, C. S. (2022). Recycling of phosphogypsum and red mud in low carbon and green cementitious materials for vertical barrier. *Sci Total Environ*, 838, 155925. [\[CrossRef\]](#)
- [25] Ghalehnovi, M., Roshan, N., Hakak, E., Shamsabadi, E. A., & De Brito, J. (2019). Effect of red mud (bauxite residue) as cement replacement on the properties of self-compacting concrete incorporating various fillers. *J Clean Prod*, 240, 118213. [\[CrossRef\]](#)
- [26] Bajpai, R., Shrivastava, A., & Singh, M. (2020). Properties of fly ash geopolymer modified with red mud and silica fume: A comparative study. *SN Appl Sci*, 2, 1–16. [\[CrossRef\]](#)
- [27] Wang, S., Jin, H., Deng, Y., & Xiao, Y. (2021). Comprehensive utilization status of red mud in China: A critical review. *J Clean Prod*, 289, 125136. [\[CrossRef\]](#)
- [28] Zhao, R., Zhang, L., Guo, B., Chen, Y., Fan, G., Jin, Z., Guan, X., & Zhu, J. (2021). Unveiling substitution preference of chromium ions in sulphoaluminate cement clinker phases. *Compos B Eng*, 222, 109092. [\[CrossRef\]](#)
- [29] Luo, S., Liu, M., Yang, L., Chang, J., Yang, W., Yan, X., Yu, H., & Shen, Y. (2019). Utilization of waste from alumina industry to produce sustainable cement-based materials. *Constr Build Mater*, 229, 116795. [\[CrossRef\]](#)
- [30] Danner, T., & Justnes, H. (2020). Bauxite residue as supplementary cementitious material—efforts to reduce the amount of soluble sodium. *Nord Concr Res*, 62(1):1–20. [\[CrossRef\]](#)

- [31] Manfroi, E. P., Cheriaf, M., & Rocha, J. C. (2014). Microstructure, mineralogy and environmental evaluation of cementitious composites produced with red mud waste. *Constr Build Mater*, 67, 29–36. [CrossRef]
- [32] Liu, X., Zhang, N., Sun, H., Zhang, J., & Li, L. (2011). Structural investigation relating to the cementitious activity of bauxite residue – Red mud. *Cem Concr Res*, 41(8), 847–853. [CrossRef]
- [33] ASTM C150/C150M-16e1 (2016) *Standard specification for Portland cement*. ASTM International.
- [34] BIS, IS 383-2016 (2016) *Specification for coarse and fine aggregates from natural sources for concrete*. Bureau of Indian Standards.
- [35] Wu, C. S., & Liu, D. Y. (2012). Mineral phase and physical properties of red mud calcined at different temperatures. *Journal of Nanomaterials*, 2012, 1–6. [CrossRef]
- [36] ASTM C109/C109M. (2022). *Standard Test Methods for Compressive Strength of Cement Mortar*. ASTM International.
- [37] ASTM C31/C31M. (2019). *Standard Practice for Making and Curing Concrete Test Specimens in the Field*. ASTM International.
- [38] ASTM C311/C311M. (2022). *Standard Test Methods for Sampling and Testing Fly Ash or Natural Pozzolans for Use in Portland-Cement Concrete*. ASTM International.
- [39] Nath, H., Sahoo, P., & Sahoo, A. (2015). Characterization of red mud treated under high-temperature fluidization. *Powder Technol*, 269, 233–239. [CrossRef]
- [40] BIS (Bureau of Indian Standards) IS: 4031 (Part 11):1988. *Method of Physical Test for Hydraulic Cement (Determination of Density)*. Bureau of Indian Standards.
- [41] Zhang, Y. N., & Pan, Z. H. (2005). Characterization of red mud thermally treated at different temperatures. *J Jinan Uni Sci Technol*, 19(4), 293–297.
- [42] Wang, P., & Liu, D. Y. (2012). Physical and chemical properties of sintering red mud and Bayer red mud and the implications for beneficial utilization. *Materials*, 5(10), 1800–1810. [CrossRef]
- [43] Meher, S. N., & Padhi, B. (2014). A novel method for the extraction of alumina from red mud by divalent alkaline earth metal oxide and soda ash sinter process. *Int J Environ Waste Manag*, 13(3), 231–245. [CrossRef]
- [44] Wang, Y., Burris, L., Shearer, C. R., Hooton, D., & Suraneni, P. (2021). Strength activity index and bulk resistivity index modifications that differentiate inert and reactive materials. *Cem Concr Compos*, 124, 104240. [CrossRef]
- [45] Kumar, K. S., Rao, M. S., Reddy, V. S., Shrihari, S., & Hugar, P. (2023). *Effect of particle size of colloidal nano-silica on the properties of the SCM based concrete*. EDP Sciences. [CrossRef]
- [46] Madhavi, C., Reddy, V. S., Rao, M. S., Shrihari, S., Kadhim, S. I., & Sharma, S. (2023). *The effect of elevated temperature on self-compacting concrete: Physical and mechanical properties*. EDP Sciences. [CrossRef]
- [47] Rossignolo, J. A. (2009). Interfacial interactions in concretes with silica fume and SBR latex. *Constr Build Mater*, 23(2), 817–821. [CrossRef]
- [48] Chand, S. R. M., Kumar, R. P., Swamy, P. N. R. G., & Kumar, G. R. (2018). Performance and microstructure characteristics of self-curing self-compacting concrete. *Adv Cem Res*, 30(10), 451–468. [CrossRef]
- [49] Venkatesh, C., Nerella, R., & Chand, M. S. R. (2021). Role of red mud as a cementing material in concrete: A comprehensive study on durability behavior. *Innov Infrastruct Solut*, 6(1), 13. [CrossRef]